Chapter 6
From Polymer Blends to Nano-size Materials with Controlled Nanomorphology

Stoyko Fakirov

Introduction

Although nanoparticles are generally considered a discovery of modern science, they actually have a very long history. Nanoparticles were used by artisans as far back as the ninth century in Mesopotamia for generating a glittering effect on the surface of pots. The peculiarities of nanomaterials arise mainly from their sizes and for this reason the search of methods for their preparation is of increasing importance.

Nanomaterials are materials with morphological features on the nanoscale, and especially those that have special properties stemming from their nanoscale dimensions. Nanoscale is usually defined as smaller than a one-tenth of a micrometer in at least one dimension [1]. In 2011 the European Commission adopted the following definition of a nanomaterial: "… 50 % or more of the particles in the number size distribution, one or more external dimensions is in the size range 1–100 nm…." [2].

An important aspect of nanotechnology is the vastly increased ratio of surface area to volume present in many nanoscale materials. For example, 1 kg of particles of 1 mm^3 has the same surface area as 1 mg of particles of 1 nm^3. The interesting and sometimes unexpected properties of nanoparticles are, therefore, largely due to the large surface area of the material, which dominates the contributions made by the small bulk of the material.

Nanoparticles may or may not exhibit size-related properties that differ significantly from those observed in fine particles or bulk materials. Although the size of most molecules would fit into the previous outline, individual molecules are usually not referred to as nanoparticles.

S. Fakirov (✉)
Department of Mechanical Engineering, Centre for Advanced Composite Materials, The University of Auckland, Private Bag 92019, Auckland, New Zealand
e-mail: s.fakirov@auckland.ac.nz

S. Fakirov (ed.), *Nano-size Polymers*,
DOI 10.1007/978-3-319-39715-3_6

Nanoparticles of usually yellow gold and gray silicon are red in color. Gold nanoparticles melt at much lower temperatures (300 °C for 2.5 nm size) than the gold slabs (1064 °C) [3]. Also, the absorption of solar radiation in photovoltaic cells is much higher in materials composed of nanoparticles than it is in thin films of continuous sheets of material (i.e., the smaller the particles, the greater the solar absorption).

Another example being closer to the topic of the present study is the polymer nanocomposites. Clay nanoparticles when incorporated into polymer matrices increase reinforcement, leading to stronger plastics, verifiable by a higher glass transition temperature and other mechanical property tests. These nanoparticles are hard, and impart their properties to the polymer. For example, with tensile moduli in the tera-pascal range and lengths exceeding 10 μ of carbon nanotubes (CNTs), simple composite models predict order-of-magnitude enhancement in modulus at loadings less than 1 %. For this reason, a decade ago it was believed that the most common polymer composites comprising about 30 % glass fibers will be replaced by the nanocomposites having only 2–5 % nano-size filler as reinforcement! Unfortunately, with the exception of reinforced elastomers, nanocomposites have not lived up to expectations [4].

Nanoparticle research is currently an area of intense scientific interest due to the wide variety of potential applications in biomedical, optical, and electronic fields.

There are several methods for creating nanoparticles, including both attrition and pyrolysis. In attrition, macro- or microscale particles are ground in a ball mill, a planetary ball mill, or other size reducing mechanism. The resulting particles are air classified to recover nanoparticles. In pyrolysis, a vaporous precursor (liquid or gas) is forced through an orifice at high pressure and burned. The final solid is air classified to recover oxide particles from by-product gases. Pyrolysis often results in aggregates and agglomerates rather than single primary particles.

Another method is the sol–gel process (also known as chemical solution deposition) widely used recently in the fields of materials science. Such methods are used primarily for the fabrication of materials (typically a metal oxide) starting from a chemical solution, which acts as the precursor for an integrated network (or gel) of either discrete particles or network polymers.

As a matter of fact, just for polymers since the beginning of the last century exists a technique for converting many polymers into nanofibrillar state using their solutions or melts. Electrospinning was first observed by Rayleigh in 1897 [5], studied further by Zeleny in 1914 [6] and patented by Formhals in 1934 [7]. Electrospinning has been widely used in the past decade to produce nanofibers from a variety of different polymers [8, 9] with a particular application in the regenerative medicine [10].

Nowadays, the electrospinning is used in hundreds of labs worldwide because of its elegancy and the fascinating electron microscopic images of the nanofibers obtained which can be seen in some 1000 papers published per year [9]. In the same time, this attractive technique has the disadvantage that not so much can be done practically with the fine nanofibers because of the not easy handling of the spun material [8–10]. In addition, this technique has another peculiarity—among the

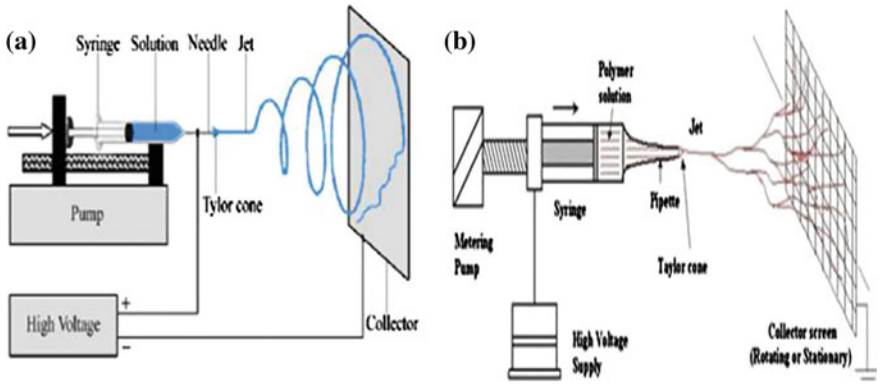

Fig. 6.1 Schematic the electrospinning setup illustrating the two different mechanisms of nanofiber formation. Reproduced with permission from Ref. [64]; Copyright 2015 Elsevier

electrospinning community there is still no consensus regarding the mechanism of nanofibre formation. As depicted in Fig. 6.1, there are two rather different mechanisms for nanowires formation. According to the first one (Fig. 6.1a), the nanowire represents a single filament, while according to the second one (Fig. 6.1b), the nanofibers are interconnected similarly to a spider network. Possibly, the answer could be found in the comparison of electrospinning with the natural silk formation and production.

After growing enough for a month, each caterpillar begins spinning a cocoon by moving its head in a pattern. Two glands produce liquid silk and force it through openings in the head (spinnerets). By the way, the misleading interpretation of the filament formation mechanism, i.e., pressing instead of drawing as later established, resulted some 150 years ago in the creation of the industry for artificial silk (rayon, viscose) [11]. Liquid silk is coated in sericin, a water-soluble protein, and solidifies on contact with air. Within 2–3 days, the caterpillar spins about 1.5 km of filament and is completely encased in a cocoon. Harvested cocoons are then soaked in boiling water to soften sericin holding the silk fibers together in a cocoon shape. The fibers are then unwound to produce a continuous tread. Since a single filament is too fine and fragile for commercial use, anywhere from three to ten strands are spun together to form a single tread of silk [12].

It seems important to mention an interesting detail regarding the structure of the cocoon and that of the electrospun material—from textile point of view both of them represent a nonwoven textile. The fact that only from a cocoon it is possible to unwound single filament is in favor of the second mechanism of nanofiber formation (Fig. 6.1b), i.e., the final electrospun product represents interconnected nanofibers similarly to the case of spider network.

The main target of this chapter is to describe a relatively new technique for converting of bulk polymers into nano-size materials with controlled nanomorphology, which does not suffer from the disadvantages of the electrospinning. The second target is to demonstrate that the final nanomorphology—individual

non-interconnected nanofibrils or three dimensional (3-D) nanoporous nanofibrillar network—can be reliably governed via presence or absence of H-bonding between the partners of the starting polymer blend. Finally, it will be shown that the offered technology for preparation of nano-sized polymers is environmentally friendly because the only solvent used could be water allowing to recycle and to reuse the second blend component for the same purpose.

Manufacturing of Nano-size Materials and Articles via the MFC Concept

Opportunities for converting the bulk polymers into nano-size materials are also offered by the developed during the last two decades new type of polymer–polymer composite, the microfibril- or nanofibril reinforced composites (MFCs or NFCs) [13–28]. MFCs and NFCs are comprised of a polymer with a lower melting temperature (T_m) as a matrix, reinforced with extremely thin fibrils of a higher T_m polymer. They are manufactured from polymer blends. The two basic requirements to the blend partners are: (i) the two polymers should not be thermodynamically miscible, and (ii) they should be easily convertable in a highly oriented state [22]. After melt blending the polymer blend is extruded, and the resulting material is then drawn, thus transforming the minor component into a fibrillar state.

In case the final target is the preparation of nanofibrillar polymer–polymer composite, a thermal treatment between the melting points of the two polymers converts the lower T_m component (the matrix) into isotropic state, while leaving the reinforcing fibrils intact. In such cases an additional requirement to the blend partners exists—a difference in their melting temperatures of at least 40 °C. MFCs and NFCs created in this way have several advantages over composites with macro-size reinforcements, the most important of which is the fact that the dispergation stage (introducing and homogenation of the reinforcing component in the matrix) is missing since the reinforcing element (fibrils) are created during the manufacturing process.

The manufacturing process for converting the bulk polymers into nano-size material can be divided into two distinct steps:

- *Mixing and extrusion*: the matrix and reinforcing polymers are dried and mixed, before being compounded and extruded. This forms an isotropic, continuous blend filament (Fig. 6.2a).
- *Drawing with fibrillation*: the blend filament is drawn through pairs of rollers (Fig. 6.2b). This step creates highly oriented micro- or nanofibrils with properties biased predominantly along a linear dimension or symmetry axis. The drawing ratio is defined as the ratio of the linear speeds (S_2/S_1) of the two sets of rollers used to draw the filament (Fig. 6.2) and gives an indication as to the amount of alignment imparted to the blend. Next, the filament is either collected on a spool or pelletized in dependence of the further type of processing, i.e., compression molding or injection molding, respectively (Fig. 6.2a).

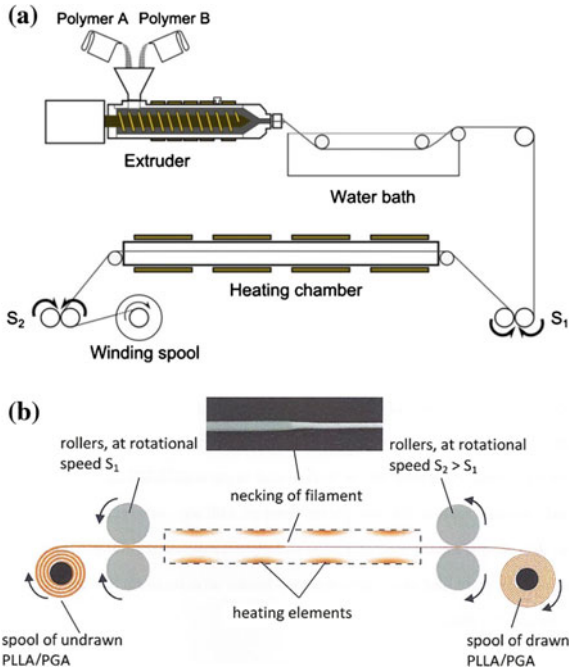

Fig. 6.2 Schematic the setup for manufacturing of MFCs (**a**) and the drawing device in more details demonstrating the neck formation (**b**); S_1 and S_2 are the rotating velocities of the pairs of rolls, where $S_1 < S_2$ and PLLA/PGA means blend of poly(L-lactic acid) and poly(glycolic acid)

Two different in situ fibril formation techniques can be employed to create the reinforcing microfibrils: (i) *cold drawing* of the solidified filament at a temperature far below the melting temperature of each blend constituent but still above their glass transition temperatures (T_g) [13–30], or (ii) *hot stretching* directly from the melt at a temperature far above both polymers' glass transition temperatures [31–39]. Cold drawing generally results in a greater molecular alignment within the microfibrils, but hot stretching can produce much higher draw ratios (although these ratios are not analogous with better molecular orientation). The drawing at temperatures around T_g takes place via the *necking phenomenon* as demonstrated in Fig. 6.2b, thus contrasting the case of hot stretching where the elongation does not require fundamental conformational changes resulting in stretching and parallel alignment of macromolecules.

The drawing performed slightly above the T_g of the reinforcing component (e.g., around 70 °C for poly(ethylene terephthalate) (PET) of the most studied polypropylene (PP)/PET blend) results in a perfect molecular orientation of the two blend partners as can be concluded from the wide-angle X-ray scattering (WAXS) patterns shown in Fig. 6.3.

At this point an important detail needs a clarification. For the cases when the target is converting a bulk polymer into nano-size material, i.e., isolation of neat nanofibrils, it is not necessary to perform the last (isotropization) step, which leads to preparation of polymer–polymer composite. In case this has to be done one has

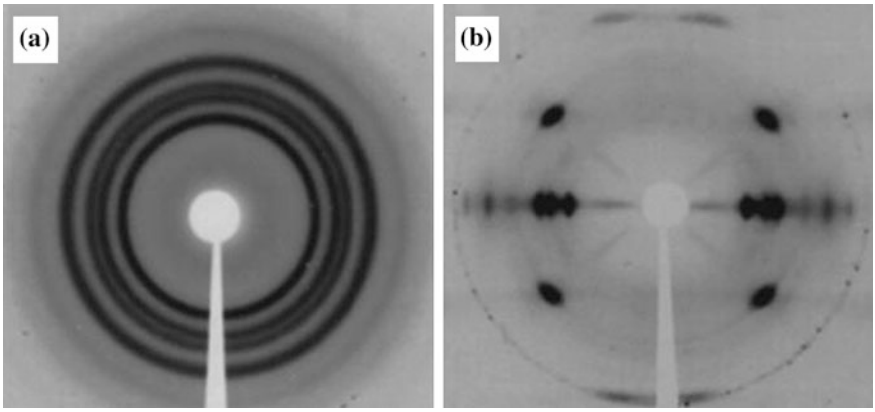

Fig. 6.3 WAXS patterns of PP/PET blends: **a** after extrusion (no drawing) and **b** after drawing. Reproduced with permission from Ref. [64]; Copyright 2015 Elsevier

to use the compression molding where aligned highly stretched drawn filaments from the polymer blend are used. During this heat treatment the lower melting component melts but the fibrils remain unchanged, even highly aligned.

For the isolation of the neat nanofibrils one can use the two rather different materials—the highly drawn polymer blend or the sheet (film) after compression molding. Either of these two materials has to be subjected to extraction of the major component using selective solvent. The rest represents parallel aligned neat nano- or microfibrils.

The extraction is a very important step of the technology. If organic solvent is used as selective solvent, the extraction has to be done at elevated temperature for many hours. The extraction time can be drastically reduced if one uses the recently modified Soxhlet apparatus [40] allowing extraction with boiling solvent.

The isolated in the described way neat micro- or nanofibrils can be further used as a starting material for manufacturing of micro-/nanofibrillar single polymer composites, as scaffolds in the regenerative medicine, as carriers for controlled drug delivery, as nanofilter and others.

Effect of Hydrogen Bonding in Polymer Blends on Nanomorphology

Non-hydrogen Bonding Polymers

To the best studied blends of this group of polymers belong the blends of polyolefins (not comprising functional groups) with condensation polymers (e.g., polyesters). In order to obtain a final product in the form of neat nanofibrils two

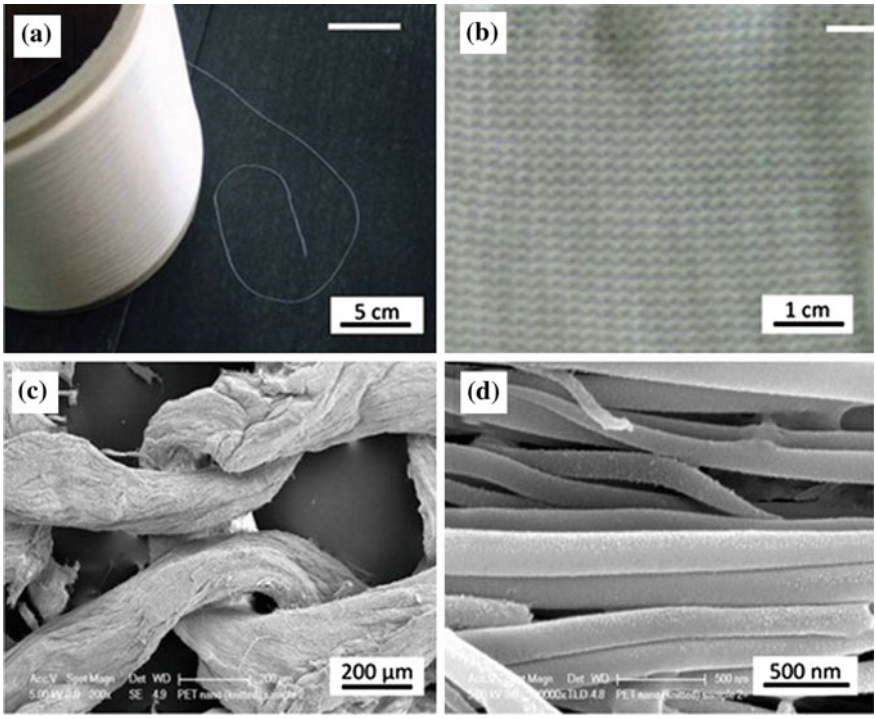

Fig. 6.4 Photograph of a PP/PET yarn of filaments with diameters of 30 µm (**a**), knitted fabrics of PP/PET yarn (**b**) and SEM micrographs of the same fabrics after removing of PP with xylene, i.e., fabrics comprising PET nanofibrils only at lower (**c**) and higher (**d**) magnifications. Reproduced with permission from Ref. [80]; Copyright 2015 Taylor & Francis

practical approaches have to be taken into account, namely: (i) intensive melt mixing leading to fine dispersion of the minor blend component, and/or (ii) using drawing conditions resulting in perfect molecular orientation. A good example for the effect of orientation could be the preparation of PET nanofibrils (Fig. 6.4).

After drying, melt blending and palletizing the PP/PET blend (80/20 wt%) was subjected to spinning using commercial equipment for manufacturing of synthetic fibers (Fig. 6.4a) thus preparing yarn of filaments with diameters of 30 µm. The final nanomaterial represents smooth not interconnected nanofibrils with thickness in the range of 50–150 nm, Fig. 6.4d. Figure 6.4 demonstrates also another peculiarity of this method of converting bulk polymers into nano-size materials—its applicability to any textile technique for manufacturing of the final articles comprising nanofibrils only. As a matter of fact, the article (Fig. 6.4b) is prepared from highly drawn polymer blend (textile yarn) and after removing of the dominating blend component (matrix) remain the nanofibrils only (Fig. 6.4d) organized in the desired way (Fig. 6.4d).

The importance of the good blend homogenization is demonstrated by the next PP/poly(butylene terephthalate) (PBT) blend. After drying and mixing (PP/PBT in

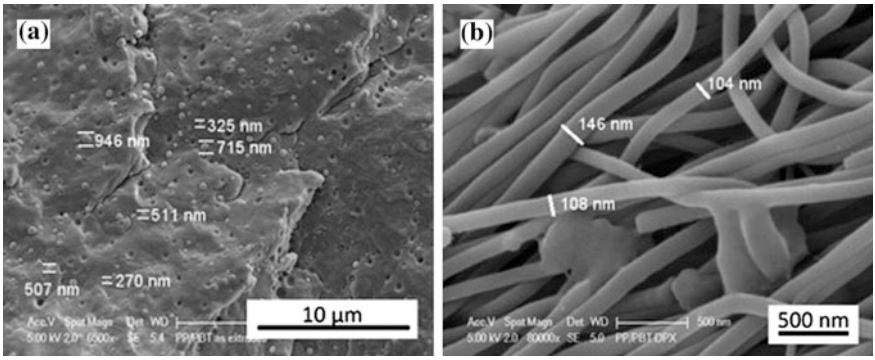

Fig. 6.5 SEM micrographs of PP/PBT blend **a** after exit from die of extruder (no drawing), and **b** after removal of PP from cold-drawn PP/PBT blend. Reproduced with permission from Ref. [80]; Copyright 2015 Taylor & Francis

weight ratio of 70/30) the melt blending was performed using a Brabender DSE20 extruder with a 25 mm screw and L/D ratio of 40, at 250 °C and 5 rpm, using a 1.3 mm die. The extrudate was cooled using a water bath immediately after its exit from the die (Fig. 6.2a). Sample of this non-drawn material was inspected in the SEM. It turned out that PBT is dispersed in the PP matrix as very fine spheres with diameters in the range of 300–700 nm (Fig. 6.5a). It is worthwhile to notice that in this particular case the smaller particles dominate. This fine dispersion of PBT in PP enhances drastically the preparation of rather thin (diameters around 100 nm) nanofibrils (Fig. 6.5b).

The extruded blend was subjected to cold drawing at 80 °C, to a ratio of about 5, using two pairs of rollers and a 2 m long heated chamber (Fig. 6.2b). This completes the fibrillation stage in the process of nanofibril formation. In order to separate the PBT neat nanofibrils, the drawn bristle was wound uniaxially on a wire frame and wrapped tightly in steel gauze. This frame was then inserted into the container of the modified Soxhlet apparatus [40], using xylene as a solvent and running it for at least 9 h, so as to completely remove PP. The isolated nanofibrils retained enough structural integrity to be unwound from the frame. The SEM observation showed that they are very smooth cylindrical formations with rather uniform diameters of about 100 nm, Fig. 6.5b. The neat PBT nanofibrils were further used for preparation of single polymer composite via winding on a metal plate, and hot compaction at temperature nearly 10 °C below the melting peak temperature [41].

The next system used for isolation of neat nanofibrils without formation of hydrogen bonding between the blend partner is the blend of linear low density polyethylene (LLDPE) (as a matrix) and poly(vinylidene fluoride) (PVDF) (as a reinforcement) in a weight ratio of 70/30 [42]. After the melt blending the extruded bristle was drawn up to a draw ratio of approximately 6. The drawing process was performed without intermittent breaking at room temperature due to high stretching

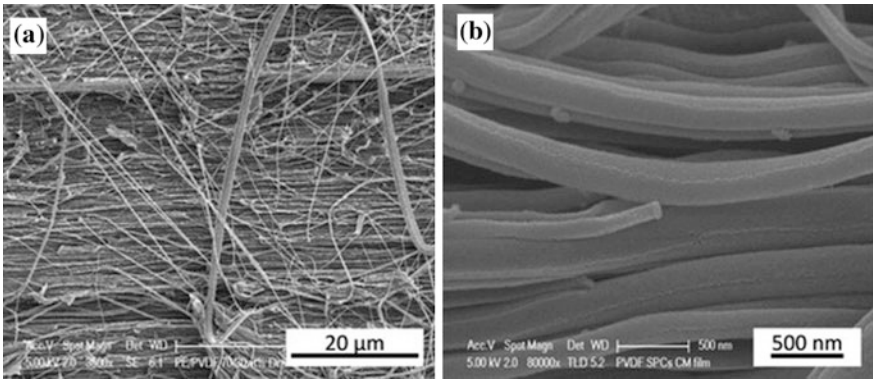

Fig. 6.6 SEM micrographs of nanofibrillar polymer–polymer composite based on LLDPE/PVDF and their reinforcing component: **a** cryofractured surface of a NFC made parallel to the draw direction, **b** neat PVDF nanofibrils after removing of LLDPE from the drawn LLDPE/PVDF blend

ability of the LLDPE. The highly drawn LLDPE/PVDF blend was wound onto a stainless steel plate and subjected to a hot pressing at 133 °C to produce a film with a NFC structure. For isolation of the PVDF neat nanofibrils the prepared nanofibrillar polymer–polymer composite (Fig. 6.6a) was subjected to extraction. The same final material (Fig. 6.6b) could be prepared if from the highly drawn blend the LLDPE will be removed using again a selective solvent.

Figure 6.6 shows SEM images of the described manufacturing stages. Figure 6.6a illustrates the perfect alignment of the reinforcing PVDF nanofibrils in the isotropic matrix of LLDPE. The same picture offers an idea about the aspect ratio of the reinforcement—nanofibrils of at least 50 µm in the length can be easily observed. Assuming an average thickness of the same nanofibrils of 100 nm (Fig. 6.6b), the aspect ratio will be of 500. Similarly to the previous SEM micrographs [12, 21, 26–28], these ones also demonstrate the very important fact—each nanofibril is surrounded individually by matrix material thus assuring a perfect dispersion of the nanoreinforcement and, what is more important, also making possible isolation of neat not agglomerated nanofibrils (Fig. 6.6).

Hydrogen Bonding Polymers

These blends are characterized by two peculiarities arising from the dominating second blend component, namely poly(vinyl alcohol) (PVA) contrasting the former dominating component (PP): (i) PVA is capable to form H-bonds because of the presence of OH groups in its molecule, and (ii) PVA belongs to the group of the few water-soluble polymers, and thus, for its extraction from the drawn blend it is not necessary to use organic solvent. To this rather new development of the method one has to come because of the application of micro- and nanofibrillar materials in

medicine (e.g., tissue engineering) where even traces of organic solvents in the scaffolds have a negative effect on the cell growth. By replacing of organic solvents with water the method became environmentally friendly, cost effective (the water-soluble polymer can be regenerated and reused for the same purpose), and, last but not least, the final nanoarticles became more attractive for biomedical applications.

The first blend of this group is that of PVA/PETG. PETG being a glycol containing copolymer of PET is characterized by lower T_m as compared with PET and thus making possible the melt blending with the temperature sensitive PVA. Further, the most important characteristic feature of these two polymers is their capability to form H-bonds between the carbonyl group =CO of the polyester and the hydroxyl group –OH of PVA. Using the already developed technique for drying (being particularly essential for the polyesters), melt blending (in a wt ratio 70/30 = PVA/PETG) with extrusion, cold drawing and extraction of PVA with water, a nano-size material is prepared, as shown in Fig. 6.7.

Figure 6.7a shows that the final material looks as a thin continuous film, and only at high magnifications it became clear that one deals with a 3-D nanofibrillar nanoporous network (Fig. 6.7b), i.e., we observe a completely different nanomorphology as compared with the cases when no H-bonding is possible (Figs. 6.4, 6.5 and 6.6).

Before considering the reasons for formation of these two rather different types of nanomorphology, namely not interconnected smooth individual nanofibrils (Figs. 6.4, 6.5 and 6.6) or 3-D nanofibrillar nanoporous network (Fig. 6.7b) let notice that the second type of morphology has been also observed for other polyesters blended with PVA (Fig. 6.8).

Starting from the respective blends, the PVA/poly(lactic acid) (PLA), PVA/poly (capro lacton) (PCL), and PVA/poly(hydroxybutyrate) (PHB), and applying the standard treatment including extraction of PVA with water, the 3-D structures have been observed (Fig. 6.8).

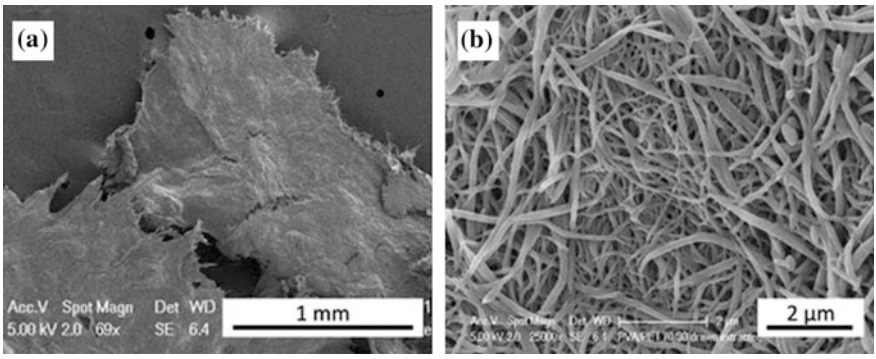

Fig. 6.7 SEM micrographs of 3-D nanofibrillar nanoporous network of PVA/PETG (70/30) blend after extrusion, cold drawing and extraction with WATER at **a** low and **b** high magnification

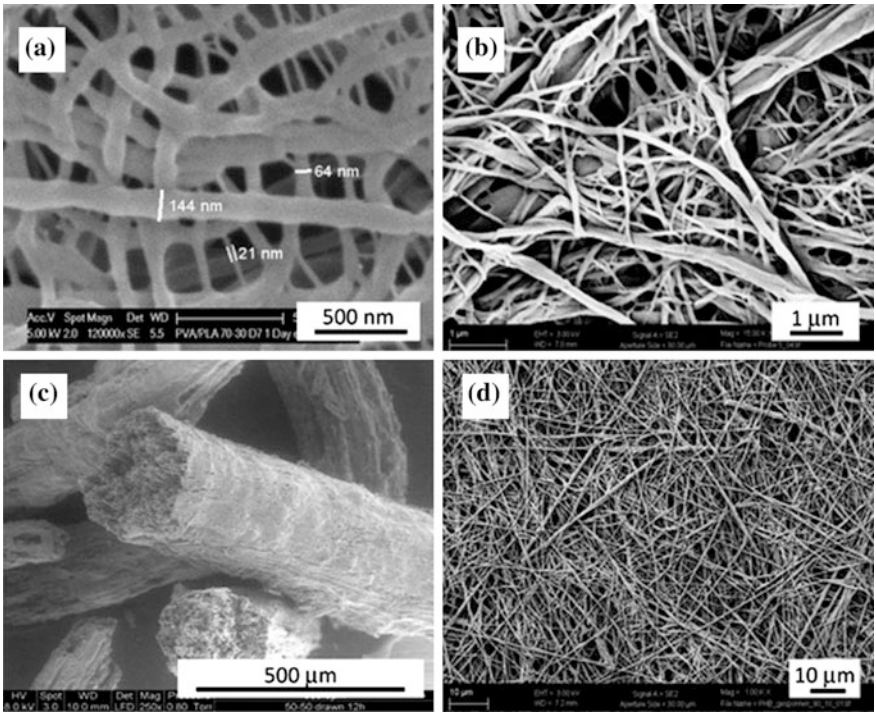

Fig. 6.8 SEM micrographs of biocompatible biodegradable polyesters after their melt blending with PVA with extrusion, cold drawing and extraction with water: **a** PLA in amount of the blend 20 wt%, **b** PCL of 20 wt%, **c** PHB after melt spinning from a PVA/PHB blend 90/10 by wt, and **d** the same at higher magnification. Reproduced with permission from Ref. [80]; Copyright 2015 Taylor & Francis

Comparing the results of the above described two types of experiments an interesting question arises: what could be the reason for obtaining of two completely different nanomorphologies of the nano-size polyesters when blended with PVA as a second blend component or with polyolefines (PP or PE)? The further systematic studies led to the conclusion that the main factor determining the type of the final nanomorphology is the possibility for formation of hydrogen bonds between the blend partners. In the cases when no hydrogen bonds exist the isolated neat nano-size materials represent individual non-interconnected fibrils and if hydrogen bonds are formed between the two blend partners the final morphology looks as a three-dimensional nanofibrillar nanoporous network.

Figure 6.9 demonstrates in the best way the crucial importance of the hydrogen bonding in polymer blends for obtaining of one or another nanomorphology because in this particular case the same polymer (PBT) has been blended with a H-bonding partner (PVA) and later with a non-hydrogen bonding partner (PP).

When H-bonding is possible as in the case of the blend PVA/PETG (Fig. 6.7) as well as in the blends of PLA, PHB, and PCL with PVA (Fig. 6.8) the final material

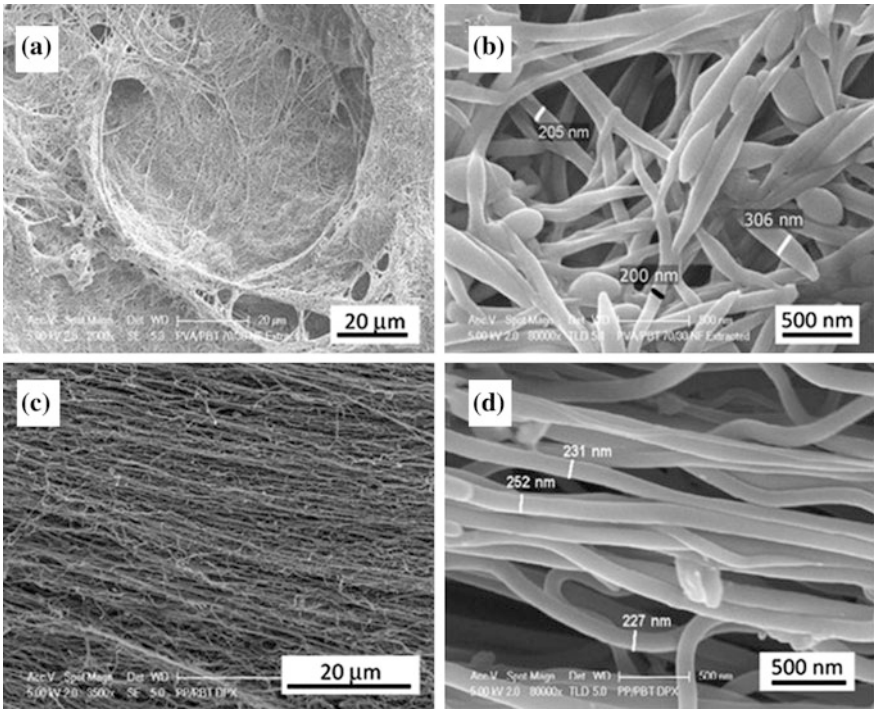

Fig. 6.9 SEM micrographs of PBT nanomorphology after removing of the second blend component: **a** and **b** PVA, **c** and **d** PP. Reproduced with permission from Ref. [80]; Copyright 2015 Taylor & Francis

is characterized by a 3-D structure (Fig. 6.9a, b) comprising nanopores and interconnected nanofibrils with diameters of about 200 nm (Fig. 6.9b). If the two blend partners are not capable to form hydrogen bonds as the case of the majority of studied blends (Figs. 6.4, 6.5 and 6.6) the final material is in the form of individual non-interconnected nanofibrils. Just the same situation one observes with the blend of PBT with PP (Fig. 6.9c, d), where the final nanomorphology represents continuous, not interconnected individual nanofibrils with diameter of about 250 nm (Fig. 6.9d). It should be noticed also that Fig. 6.9 demonstrates not only the importance of H-bonding for the formation of the final nanomorphology but also the potentials of the suggested method for converting of bulk polymers into nano-size materials with controlled nanomorphology. As a matter of fact, starting from the same bulk polymer (PBT) we are able to prepare two nano-size materials characterized by rather different nanomorphology, namely as individual not interconnected nanofibrils or as 3-D nanofibrillar nanoporous network.

Figure 6.10 shows schematically the formation of hydrogen bonds between polyesters and PVA.

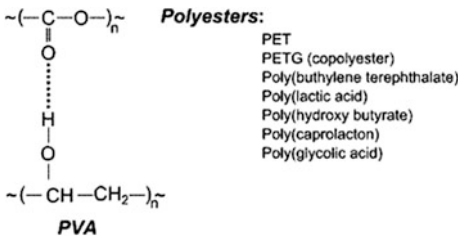

Fig. 6.10 Hydrogen bonding between polyesters and poly (vinyl alcohol)

Hydrogen bonding in polymer blends is a topic of great interest to polymer scientists because such systems have many potential applications [43–48]. For example, introducing functional groups to one component to make it capable of forming hydrogen bonds to another, thereby enhancing miscibility of otherwise immiscible blends, is one of the major achievements during the past 20 years of polymer science, as stated in a recent review on hydrogen bonding in polymer blends [49].

Coming back to our particular systems, the blends of PVA with various polyesters, one can assume that one deals with partial solubility leading to a good compatibilization of the two polymers due to the formation of H-bonds between them (Fig. 6.10). Existence of a complete solubility (thermodynamic miscibility) is excluded because in such a case one will obtain a one-phase melt. On the contrary, the partial solubility provoked by the H-bonding is the driving force for penetrating a small amount of the dominating component (PVA) in the dispersed particles of the minor component (e.g., PLA), forming a structure consisting of two co-continuous phases. After the extraction of this small amount finely dispersed PVA, a 3-D network of micro- or nanopores is formed (Figs. 6.7b, 6.8 and 6.9a, b). This assumption [50] is supported by the observation that in a ternary blend of poly (vinyl butyral)/PVA/PA 6, a thermodynamic miscibility of 0.4–0.6 volume fraction of vinyl alcohol has been found [51]. The SEM inspection of this blend after selective extraction of the dissolved component revealed a network of micropores [51, 52].

For a system much closer chemically and compositionally to PVA/PLA, Park and Im [53] reported that PLA/poly(vinyl acetate) (PVAc) blends were miscible systems for the entire composition range, but for the blends with even 10 % hydrolyzed PVAc copolymer, the phase separation and double glass transition could be observed. Another thorough study [54] on miscibility and phase structure of binary blends of poly(L-lactic acid) (PLLA) and PVA indicated that PLLA and PVA were immiscible in the amorphous regions. However, the data of the differential scanning calorimetry analysis still demonstrated that some degree of compatibility related to block composition existed in the blend systems. Furthermore, the formation of interpolymer hydrogen bonding in the amorphous region which is regarded as the driving force leading to some degree of component compatibility in these immiscible systems, has been confirmed by FTIR and further studied by ^{13}C solid-state NMR analysis [54].

Obviously, the hydrogen bonding is a powerful tool for controlling the properties of polymer blends, and more specifically the nanomorphology when converting the bulk polymers into nano-size materials. Blending completely immiscible polymers and applying the MFC concept makes possible the isolation of nano-size material in the form of individual not interconnected nanofibrils. In contrast to this situation, dealing with blend partners inclined to formation of hydrogen bonds and thus converting the blend in a partially miscible one the final nano-size material is a nanofibrillar nanoporous 3-D network.

Mechanism of Nanomorphology Formation in Polymer Blends Without and with Hydrogen Bonding

In addition to the outlined morphological difference between the two types of polymer blends, without and with hydrogen bonding between the blend partners, it turned out that the mechanism of formation of the nano-size materials is completely different for the one or the other case. Detailed studies on the mechanism of formation of the individual micro- and nanofibrils led to the conclusion that it takes place during the cold drawing via *coalescence* of the elongated droplets [55], as schematically illustrated in Fig. 6.11.

The rare statements (e.g., [56]) that each final fibril originates from a single spherical particle could hardly be correct for the following reasons: the comparison of the volumes of a starting sphere with that of the final fibril shows difference of many tens in favor of the fibril; further on, the draw ratio is typically around 5 and never higher than 10 (i.e., the starting spheres will be converted in particles with

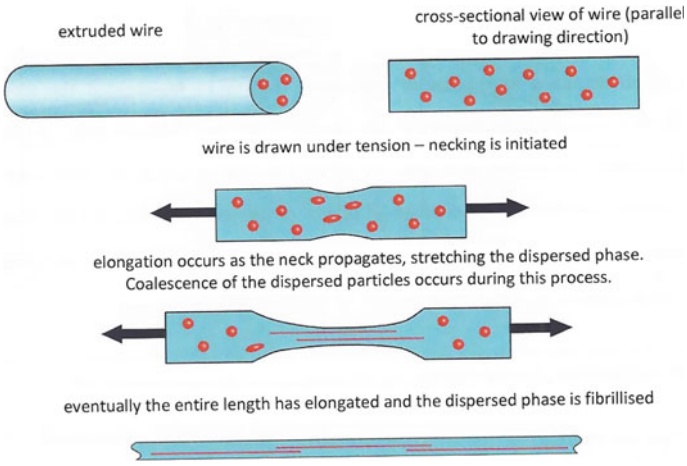

Fig. 6.11 Schematic the microfibril formation mechanism in polymer blends without hydrogen bonding during cold drawing (transformation of the spherical particles into microfibrils via coalescence under transverse contraction)

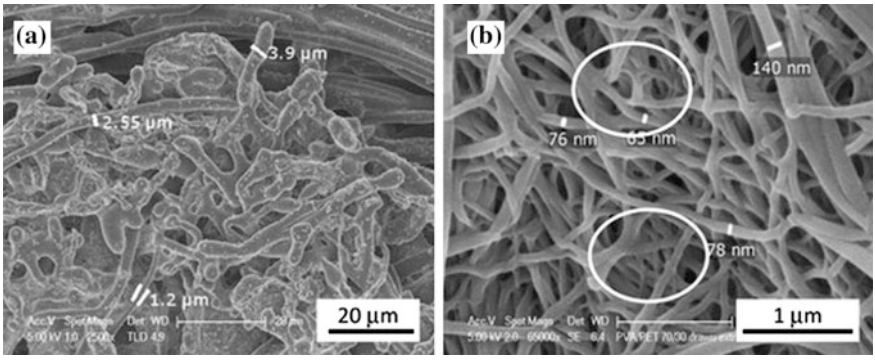

Fig. 6.12 SEM micrographs of PVA/PETG blend (70/30 wt%) taken after melt blending and extraction of PVA with water: **a** the sample is taken just after the die (no cold drawing) and **b** the sample is taken after the cold drawing. Reproduced with permission from Ref. [64]; Copyright 2015 Elsevier

maximum 10 times larger length but not 100 times as it follows from the final length of fibrils).

Systematic study of the mechanism of formation of the 3-D network in the case of polymer blends with H-bonding demonstrated that this process takes place in the melt *before* the drawing step. The subsequent cold drawing results in drastic reduction of the diameters of the network's fibrillar elements. This conclusion was proved by SEM observation of melt blended samples taken immediately after the extruder die. They were treated with water in order to extract the PVA and analyzed by SEM. The results are displayed in Fig. 6.12.

Figure 6.12a shows that the formation of the basic structure takes place in the extruder where the two partners are in a molten state, which favors the formation of H-bonds for the following reasons. In the melt the polymer chains are more flexible and mobile and additionally agitated by the rotating screw thus contributing to the intimated mixing of the two blend components and establishing of maximum H-bonds. The arising structure of the blend is of the type of two co-continuous phases, which is stabilized by the established H-bonds and further fixed by the subsequent cooling to room temperature. An important characteristic of this 3-D network is the thickness of its elements—their diameters are in the range of a couple of microns (Fig. 6.12a).

What happens during the cold drawing? First of all, the character of the 3-D structure arising in the molten blend is completely preserved. The only change, which takes place, is the conversion of the *microfibrillar* 3-D network into *nanofibrillar* 3-D network (Fig. 6.12b). With the progress of cold drawing the sizes of the constituting fibrils of the 3-D network become finer approaching the nanorange as can be concluded from Fig. 6.12b. This microphotograph, taken at higher magnification (65,000×) demonstrates that the majority of nanofibrils have a diameter around 70 nm and the nanopores are typically between 50 and 200 nm in size. The same images indicate on another peculiarity of the system—the really

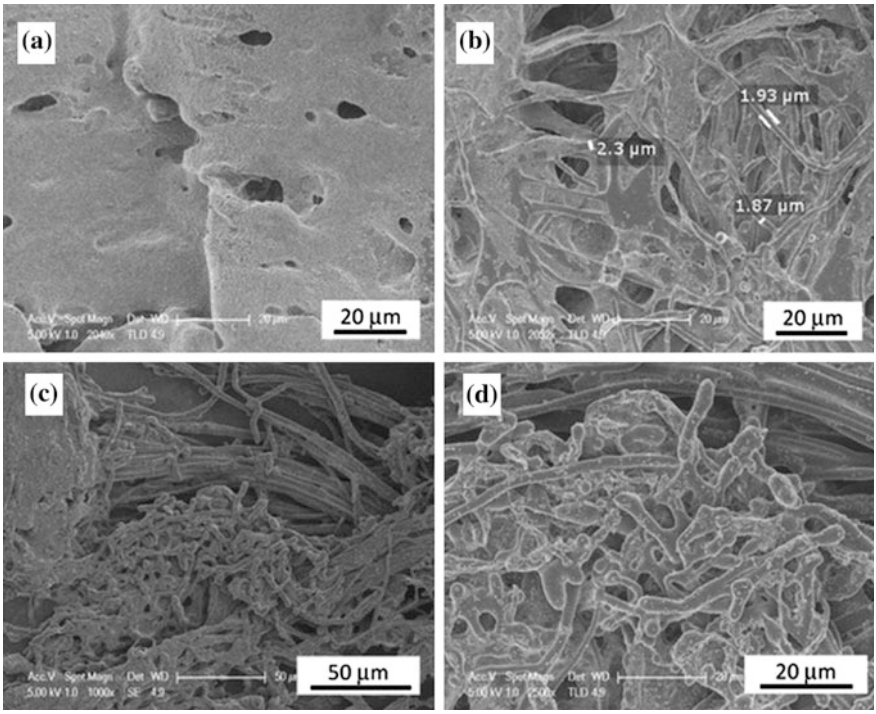

Fig. 6.13 SEM micrographs of PVA/PETG blend samples taken immediately after the die and subjected to PVA extraction with water with PVA/PETG wt ratio: **a** 30/70, **b** 50/50, **c** and **d** 70/30. Reproduced with permission from Ref. [80]; Copyright 2015 Taylor & Francis

branched character of the structure formed. Some of the branching "points" are highlighted in Fig. 6.12b using white ellipses for a better visualization.

The effect of concentration ratio of the blend components on the formation of 3-D network was also studied. For this purpose again samples just after the extruder die were taken and subjected to extraction of PVA followed by analysis using SEM. Blends of PVA/PETG in three different ratios were prepared: 30/70, 50/50, and 70/30. The respective results of SEM examination are shown in Fig. 6.13.

The microphotographs in Fig. 6.13 demonstrate that (i) the formation of a polymer blend with a co-continuous structure takes place during the melt blending, i.e., before drawing the extrudate, and (ii) the effect of the ratio of the two blend components for the formation of co-continuous phases is essential. The blend with the highest amount of PVA (70 %, Fig. 6.13c, d) is characterized by the best mutual penetrating structures with the finest fibrils as compared with the blends with less PVA (50 %, Fig. 6.13b) and particularly the case with the lowest PVA content (30 %, Fig. 6.13a). For the last case of blend composition the lack of fibrillar structures is understandable—PETG is the dominating component (70 %) in which PVA is dispersed, and using a selective for the PETG solvent it would be possible to isolate a PVA fibrillar structure (as a 3-D network in the present case).

Application Opportunities of Nano-size Polymers

Possibly, the main application of polymer nanofibrils is their use as reinforcing component of polymer nanocomposites. The most important advantage of this type of nanocomposites in comparison to the common polymer nanocomposites (prepared via blending of nano-size reinforcement with the matrix polymer) is the lack of dispersion step in their manufacturing process [28, 57–59, 61], similarly to their microfibrillar analogs [13, 24–26, 28, 30, 41, 42, 60, 61].

Quite different application opportunities are offered after the isolation of neat nanofibrils. At the first place is their usage for preparation of nanofibrillar single polymer composites (i.e., the case when the matrix and the reinforcement are of the same chemical composition). Regardless of some controversy from terminological point of view [62–64], this rather novel type of polymer composites represents possibly the best solution of the problem regarding the adhesion quality between matrix and reinforcement. In addition, recyclability after disposal is other main merit of SPCs [65].

The most recent development in the area of SPCs is the creation of micro- or nanofibrillar single polymer composites, where the starting material represents neat microfibrils or nanofibrils [21, 66–71] instead of commonly used highly oriented textile fibers and strips or their products [72–77]. This was possible due to the fact that the MFC and NFC concept allows not only to convert the dispersed polymer into highly oriented fibrils but also to isolate them as a neat material using selective solvent for removing of the second blend component [40].

Another important opportunity for the application of the polymer nano-size materials is their use for biomedical purposes. Organ transplantation nowadays practically has no technical problems. The problem is the lack of donors—only in USA alone a quarter of patients in need die while waiting for suitable donor. The solution was found in the creation of a new science, the tissue engineering, i.e., the use of a combination of cells, engineering, and materials methods to improve or replace biological functions (e.g., tissue, organs).

Cells are often implanted or "seeded" into an artificial structure capable of supporting three-dimensional tissue formation. These structures, typically called *scaffolds*, usually serve at least one of the following purposes: (i) allow cell attachment and migration, (ii) deliver and retain cells and biochemical factors, (iii) enable diffusion of vital cell nutrients and expressed products, and (iv) exert certain mechanical and biological influences to modify the behavior of the cell phase. Taking into account one of the basic requirements to the scaffolds, namely the high specific surface, which can be achieved using fibrillar and/or porous materials, it looked challenging to apply for the same purpose the concept of converting of bulk polymers into nano-size materials. Particularly attractive seemed to be the nano-size biodegradable biocompatible polymers with a 3-D network structure because of their nanoporosity and extremely high specific surface. Additional advantage of these materials is the fact that they are manufactured without any use of organic solvents since the only solvent used is water.

The results of the biomedical testing with living cells are quite promising—the cells attach rather well to the scaffold surface proliferate and grow further [52, 59, 78, 79].

Conclusions and Outlook

The peculiar properties of nanomaterials arise mainly from their sizes and for this reason the search of methods for converting the known materials into nano-size ones is of paramount importance. The electrospinning used for this purpose is simple and cost-effective method but the final product always represents a non-woven textile from nanofibers with a quite limited application potential. Contrasting to the electrospinning, the *concept of nanofibrillar composites* makes possible the application of any textile technique for preparation the respective articles starting from textile yearn of polymer blend, followed by removing of the second blend component in order to prepare articles comprising nanofibrils only (with diameters of 50–250 nm). The neat nanofibrils and articles thereof can be used as scaffolds in tissue engineering, micro- and nanofilters in industry, as starting materials for single polymer composites, as carriers for controlled drug delivery, and others. In this way it is possible to convert any bulk polymer into nano-size material. Recently, this approach was essentially improved be excluding the use of organic solvents—the only solvent used is water. In this way the method became environmentally friendly and cost-effective (the water-soluble polymer can be regenerated and reused for the same purpose), and, last but not least, the final nanoarticles became more attractive for biomedical applications.

Further development of the same method was the finding that the final nanomorphology, being of two basic types, can be controlled using hydrogen bonding as a tool for governing. If hydrogen bonding between the blend partners is missing, the observed morphology is of individual not interconnected nanofibrils. In case hydrogen bonds are present the nanomorphology represents a nanofibrillar nanoporous 3-D network.

Regarding the future trends in the area of described studies two topics of the main interest have to be mentioned: (i) elaboration of effective methods for suppressing the H-bonding of the polymer of interest in order to avoid formation of nanomorphology of network type and thus to prepare neat nano-size material with superior mechanical properties, and (ii) widening the application opportunities of the new nanomaterials and attempting their commercialization.

Acknowledgments The author would like to thank the Foundation for Research Science and Technology of New Zealand for the financial support (Grant No. UOAX 0406). He acknowledges also the hospitality of the Centre for Advanced Composite Materials at the University of Auckland where this study was completed.

References

1. Buzea C, Pacheco II, Robbie K (2007) Nanomaterials and nanoparticles: sources and toxicity. Biointerphases 2:MR17–MR71
2. http://ec.europa.eu/environment/chemicals/nanotech/faq/definition_en.htm. Accessed 20 Apr 2014
3. Buffat P, Borel J (1976) Size effect on melting temperature of gold particles. Phys Rev A 13:2287–2298
4. Schaefer DW, Justice RS (2007) How nano are nanocomposites? Macromolecules 40 (24):8501–8517
5. Bhardwaj N, Kundu SC (2010) Electrospinning: a fascinating fiber fabrication technique. Biotechnol Adv 28:325–347
6. Zeleny J (1914) The electrical discharge from liquid points, and a hydrostatic method of measuring the electric intensity at their surfaces. J Phys Rev 3(2):69–91
7. Formhals A (1934) Process and apparatus for preparing artificial threads, U.S. Patent No. 1,975,504
8. Huang ZM, Zhang YZ, Kotaki M, Ramakrishna S (2003) A review on polymer nanofibers by electrospinning and their applications in nanocomposites. Compos Sci Technol 63(15): 2223–2253
9. Greiner A, Wendorff JH (2007) Electrospinning: a fascinating method for the preparation of ultrathin fiber. Angew Chem Int Ed 46(30):5670–5703
10. Agarwal S, Wendorff JH, Greiner A (2008) Polymer 49(26):5603–5621
11. Editors (1991) Time-life, inventive genius. Time-Life Books, New York, p 52
12. Glaeson C (2007) The biography of silk. Crabtree Publishing Company, p 12
13. Fakirov S (2012) The concept of micro- or nanofibrils reinforced polymer–polymer composites. In: Bhattacharyya D, Fakirov S (eds) Synthetic polymer–polymer composites. Hanser Publisher, Munich, pp 353–400
14. Fakirov S (2013) H-bonding—a chance for novel nano-sized polymers. Expr Polym Lett 7 (6):494–494
15. Fakirov S, Evstatiev M, Schultz JM (1993) Microfibrillar reinfporced composites from drawn poly(ethylene terephthalate)/nylon blends. Macromolecules 34(22):4669–4679
16. Evstatiev M, Fakirov S, Krasteva B, Friedrich K, Covas J, Cunha A (2002) Recycling of PET as polymer–polymer composites. Polym Eng Sci 42(4):826–835
17. Fakirov S, Kamo H, Evstatiev M, Friedrich K (2004) Microfibrillar reinforced composites from PET/LDPE blends: morphology and mechanical properties. J Macromol Sci B Phys B43 (4):775–789
18. Friedrich K, Ueda E, Kamo H, Evstatiev M, Fakirov S, Krasteva B (2002) Direct electron microscopic observation of transcrystalline layers in microfibrillar reinforced polymer–polymer composites. J Mater Sci 37(20):4299–4305
19. Krumova M, Michler GH, Evstatiev M, Friedrich K, Stribeck N, Fakirov S (2005) Transcrystallization with reorientation of polypropylene in drawn PET/PP and PA66/PP blends. Part 2 Electron microscopic observations on the PET/PP blend. Prog Colloid Polym Sci 130:167–173
20. Sapoundjieva D, Denchev Z, Evstatiev M, Fakirov S, Stribeck N, Stamm M (1999) Transcrystallization with reorientation in drawn PET/PA12 blend as revealed by WAXS from synchrotron radiation. J Mater Sci 34(13):3063–3067
21. Bhattacharyya D, Maitrot P, Fakirov S (2009) Polyamide 6 single polymer composites. Expr Polym Lett 3(8):525–532
22. Evstatiev M, Fakirov S, Bechtold G, Friedrich K (2000) Structure—property relationships of injection- and compression-molded microfibrillar reinforced PET/PA-6 composites. Adv Polym Technol 19(4):249–259
23. Fakirov S, Sarac Z, Anbar T, Boz B, Bahar I, Evstatiev M, Apostolov A, Mark J, Kloczkowski A (1996) Mechanical properties and transition temperatures of crosslinked

oriented gelatin. 1. Static and dynamic mechanical properties of cross-linked gelatin. Colloid Polym Sci 274(4):334–341
24. Fakirov S, Evstatiev M (1990) New routes to poly(ethylene terephthalate) with improved mechanical properties. Polymer 31(3):431–434
25. Kargin VA, Bakeev NF, Fakirov SK (1964) New direct observation technique of structure of polymer solutions with aid of electron microscope. Dokl Acad Nauk SSSR 159(4):885
26. Fuchs C, Bhattacharyya D, Fakirov S (2006) Microfibril reinforced polymer–polymer composites: application of Tsai-Hill equation to PP/PET composite. Compos Sci Technol 66 (16):3161–3171
27. Fuchs C, Bhattacharyya D, Friedrich K, Fakirov S (2006) Application of Halpin–Tsai equation to microfibril reinforced polypropylene/poly(ethylene terephthalate) composites. Compos Interfaces 13(4–6):331–344
28. Fakirov S, Bhattacharyya D, Shields RJ (2008) Nanofibril reinforced composites from polymer blends. Coll Surf A Physicochem Eng Aspects 313–314:2–8
29. Fakirov S, Evstatiev M, Schultz JM (1993) Microfibrillar reinforced composite from drawn poly(ethylene terephthalate) nylon blends. Polymer 34(22):4669–4679
30. Fakirov S, Evstatiev M, Petrovich S (1993) Microfibrillar reinforced composites. Macromolecules 26(19):5219–5226
31. Li ZM, Huang CG, Yang W, Yang MB, Huang R (2004) Morphology dependent double yielding in injection molded polycarbonate/polyethylene blend. Macromol Mater Eng 289 (11):1004–1011
32. Li ZM, Lu A, Lu ZY, Shen KZ, Li LB, Yang MB (2005) In-situ microfibrillar PET/iPP blend via a slit die extrusion, hot stretching and quenching process: influences of PET concentration on morphology and crystallization of iPP at a fixed hot stretching ratio. J Macromol Sci Phys B44(2):203–216
33. Li ZM, Yang MB, Lu A, Feng JM, Huang R (2002) Tensile properties of poly(ethylene terephthalate) and polyethylene in-situ microfiber reinforced composite formed via slit die extrusion and hot stretching. Mater Lett 56(5):756–762
34. Li ZM, Yang MB, Xie BH, Lu A, Feng JM, Huang R (2003) In-situ microfiber reinforced composite based on PET and PE via slit die extrusion and hot stretching. Influences of hot stretching ratio on morphology and tensile properties at a fixed composition. Polym Eng Sci 43(3):615–628
35. Li ZM, Li LB, Shen KZ, Yang MB, Huang R (2004) In-situ microfibrillar PET/iPP blend via slit die extrusion, hot stretching, and quenching: influence of hot stretch ratio on morphology, crystallization, and crystal structure of iPP at a fixed PET concentration. J Polym Sci B Polym Phys 42(22):4095–4106
36. Zhong GJ, Li LB, Mendes E, Byelov D, Fu Q, Li ZM (2006) Suppression of skin-core structure in injection-molded polymer parts by in-situ incorporation of a microfibrillar network. Macromolecules 39(19):6771–6775
37. Zhong GJ, Li ZM, Li LB, Shen KZ (2008) Crystallization of oriented isotactic polypropylene (iPP) in the presence of in situ poly(ethylene terephthalate) (PET) microfibrils. Polymer 49 (19):4271–4278
38. Yi X, Xu LK, Wang YL, Zhong GJ, Ji X, Li ZM (2010) Morphology and properties of isotactic polypropylene/poly(ethylene terephthalate) in situ microfibrillar reinforced blends: influence of viscosity ratio. Eur Polym J 46(4):719–730
39. Yi X, Chen C, Zhong GJ, Xu L, Tang JH, Ji X, Li ZM (2011) Suppressing the skin–core structure of injection-molded isotactic polypropylene via combination of an in situ microfibrillar network and an interfacial compatibilizer. J Phys Chem B 115(23):7497–7504
40. Fakirov S (2006) Modified Soxhlet apparatus for high-temperature extraction. J Appl Polym Sci 102(2):2013–2014
41. Panamoottil SM, Bhattacharyya D, Fakirov S (2013) Nanofibrillar polymer–polymer and single polymer composite involving poly(butylene terephthalate): preparation and mechanical properties. Polym Plast Technol Eng 52(11):1106–1112

42. Kim NK, Bhattacharyya D, Fakirov S (2014) Polymer–polymer and single polymer composites involving nanofibrillar poly(vinylidene fluoride): manufacturing and mechanical properties. J Macromol Sci Phys B53(7):1168–1181
43. Kotek R, Tonelli A, Vasanthan N (2003) Lewis acid-base complexation of polyamides and the effect of hydrogen bonding on structure development, M01-NS03, NTC Project
44. Kotek R, Jung D, Tonelli A, Vasanthan N (2005) Novel methods for obtaining high modulus aliphatic polyamide fibers. J Macromol Sci Polym Rev C45(3):201–230
45. Kotek R, Pang K, Schmidt B, Tonelli A (2004) Synthesis and gas barrier characterization of poly(ethylene isophthalate). J Polym Sci Part B Polym Phys 42(23):4247–4254
46. Jung DW, Kotek R, Vasanthan N, Tonelli A (2004) High modulus nylon 66 fibers through Lewis acid-base complexation to control hydrogen bonding and enhance drawing behavior. 228th ACS National Meeting, Philadelphia, PA
47. Vasanthan N, Kotek R, Jung DW, Shin D, Tonelli AE, Salem DR (2004) Lewis acid-base complexation of polyamide 66 to control hydrogen bonding, extensibility and crystallinity. Polymer 45(12):4077–4085
48. Vasanthan N, Kotek R, Jung DW, Salem DR, Tonelli AE (2004) Lewis acid-base complexation of polyamide 66 as a means to control hydrogen bonding to form high strength fibers and films. 227th ACS National Meeting, Anaheim, CA
49. Kuo SW (2008) Hydrogen-bonding in polymer blends. J Polym Res 15(6):459–486
50. Fakirov S, Bhattacharyya D, Hutmacher D (2008) Applications of microfibrillar polymer–polymer composites concept for biomedical purposes. In: Bhatnagar N, Srivatsan TS (eds) Processing and fabrication of advanced materials—XVII, vol 2. IIIK International, New Delhi, pp 794–803
51. Shuai X, He Y, Asakawa N, Inoue YJ (2001) Miscibility and phase structure of binary blends of poly(L-lactide) and poly(vinyl alcohol). J Appl Polym Sci 81(3):762–772
52. Bini T, Gao S, Wang S, Ramakrishna S (2006) Poly(l-lactide-co-glycolide) biodegradable microfibers and electrospun nanofibers for nerve tissue engineering: an in vitro study. J Mater Sci 41(19):6453–6459
53. Park JW, Im SS (2003) Miscibility and morphology in blends of poly(L-lactic acid) and poly (vinyl acetate-co-vinyl alcohol). Polymer 44(15):4341–4354
54. Chiu JB, Luu YK, Fang D, Hsiao BS, Chu B, Hadjiargyrou M (2005) Electrospun nanofibrous scaffolds for biomedical applications. J Biomed Nanotechnol 1(2):115–132
55. Fakirov S, Bhattacharya D, Lin R, Fuchs C, Friedrich K (2007) Contribution of coalescence to microfibrils formation in polymer blends during cold drawing. J Macromol Sci Phys B46 (1):183–194
56. Denchev Z, Dencheva N (2012) Preparation, mechanical properties and structural characterization of microfibrillar composites based on polyethylene/polyamide blends. In: Bhattacharyya D, Fakirov S (eds) Synthetic polymer–polymer composites. Hanser Publisher, Munich, pp 465–524
57. Bhattacharyya D, Fakirov S, Organoclay (2009) Particulate and nanofibril reinforced polymer-polymer composites: manufacturing, modeling and applications. In: Karger-Kocsis, Fakirov S (eds) Nano- and micro-mechanics of polymer blends and composites. Hanser, Munich, pp 167–208
58. Shields R, Bhattacharyya D, Fakirov S (2008) Fibrillar polymer-polymer composites: morphology, properties and applications. J Mater Sci 43(20):6758–6770
59. Shields RJ, Bhattacharyya D, Fakirov S (2012) Application opportunities of the microfibril reinforced composite concept. In: Bhattacharyya D, Fakirov S (eds) Synthetic polymer–polymer composites. Hanser, Munich, pp 589–626
60. Evstatiev M, Fakirov S, Friedrich K (2000) Microfibrillar reinforced composite: another approach to polymer blends processing. In: Fakirov S (ed) Structure development during polymer processing. Kluwer Academic, Dordrecht, The Netherlands, pp 311–325
61. Evstatiev M, Fakirov S, Friedrich K (2005) Manufacturing and characterization of microfibrillar reinforced composites from polymer blends. In: Friedrich K, Fakirov S, Zhang Z (eds) Polymer composites: from nano- to macro-scale. Springer, Boston, pp 149–167

62. Fakirov S (2015) Is the use of correct terms and definitions important in creation of new materials? Expr Polym Lett 9(8):671
63. Fakirov S (2015) Composite materials—is the use of proper definitions important? Mater Today 18(10):529
64. Fakirov S (2013) Nano-/microfibrillar polymer-polymer and single polymer composites: the converting instead of adding concept. Comp Sci Technol 89:211–225
65. Matabola K, De Vries A, Moolman F, Luyt A (2009) Single polymer composites: a review. J Mater Sci 44(23):6213–6222
66. Duhovic M, Fakirov S, Holschuh R, Mitschang P, Bhattacharyya D (2012) Micro- and nanofibrillar single polymer composites. In: Bhattacharyya D, Fakirov S (eds) Synthetic polymer–polymer composites. Hanser, Munich, pp 643–672
67. Karger-Kocsis J, Fakirov S (2012) Polymorphism- and stereoregularity-based single polymer composites. In: Bhattacharyya D, Fakirov S (eds) Synthetic polymer–polymer composites. Hanser, Munich, pp 673–698
68. Fakirov S (2013) Nano- and microfibrillar single-polymer composites: a review. Macromol Mater Eng 298(1):9–32
69. Duhovic M, Maitrot P, Fakirov S (2009) Polyamide 66 polymorphic single polymer composites. Open Macromol J 3:37–40
70. Duhovic M, Bhattacharyya D, Fakirov S (2010) Nanofibrillar single polymer composites of poly(ethylene terephthalate). Macromol Mater Eng 295(2):95–99
71. Fakirov S, Duhovic M, Maitrot P, Bhattacharyya D (2010) From PET nanofibrils to nanofibrillar single-polymer composites. Macromol Mater Eng 295(6):515–518
72. Capiati NJ, Porter RS (1975) Concept of one polymer composites modeled with high-density polyethylene. J Mater Sci 10(10):1671–1677
73. Hine P, Ward I, Olley R, Bassett D (1993) The hot compaction of high modulus melt-spun polyethylene fibers. J Mater Sci 28(2):316–324
74. Hine P, Olley R, Ward I (2008) The use of interleaved films for optimising the production and properties of hot compacted, self-reinforced polymer composites. Comp Sci Technol 68 (6):1413–1421
75. Cabrera NO, Alcock B, Klompen BET, Peijs T (2008) Filament winding of co-extruded polypropylene tapes for fully recyclable all-polypropylene composite products. Appl Compos Mater 15(1):27–45
76. Li R, Yao D (2008) Preparation of single poly(lactic acid) composites. J Appl Polym Sci 10:2909–2916
77. Barkoula NM, Alcock B, Cabrera NO, Peijs T (2008) Fatigue properties of highly oriented polypropylene tapes and all-polypropylene composites. Polym Polym Compos 16(2):101–113
78. Lin STC, Bhattacharyya D, Fakirov S, Cornish J (2014) Novel organic solvent free micro-/nano-fibrillar, nanoporous scaffolds for tissue engineering. Int J Polym Mater Polym Biomater 63(8):416–423
79. Lin STC, Bhattacharyya D, Fakirov S, Matthews BG, Cornish J (2014) A novel microfibrillar composite approach towards manufacturing nanoporous tissue scaffolds. Mech Adv Mater Struct 21(3):237–243
80. Fakirov S, Bhattacharyya D, Panamoottil SM (2014) Converting of bulk polymers into nanosized materials with controlled nanomorphology. Int J Polym Mater Polym Biomater 63 (15):777–793